Absorption and resonance Raman characteristics of β-carotene in water-ethanol mixtures, emulsion and hydrogel

Merve Meinhardt-Wollweber, Christian Suhr, Ann-Kathrin Kniggendorf, and Bernhard Roth

Citation: AIP Advances **8**, 055320 (2018); doi: 10.1063/1.5025788
View online: https://doi.org/10.1063/1.5025788
View Table of Contents: http://aip.scitation.org/toc/adv/8/5
Published by the American Institute of Physics

AIP ADVANCES **8**, 055320 (2018)

Absorption and resonance Raman characteristics of β-carotene in water-ethanol mixtures, emulsion and hydrogel

Merve Meinhardt-Wollweber,[a] Christian Suhr, Ann-Kathrin Kniggendorf, and Bernhard Roth
Hannover Centre for Optical Technologies, Leibniz Universität Hannover, Nienburger Str. 17, 30167 Hannover, Germany

(Received 13 February 2018; accepted 10 May 2018; published online 21 May 2018)

Absorption or resonance Raman scattering are often used to identify and even quantify carotenoids *in situ*. We studied the absorption spectra, the Raman spectra and their resonance behavior of β-carotene in different molecular environments set up as mixtures from lipid (emulsion) and non-polar (ethanol) solvents and a polar component (water) with regard to their application as references for *in situ* measurement. We show how both absorption profiles and resonance spectra of β-carotene strongly depend on the molecular environment. Most notably, our data suggests that the characteristic bathochromic absorption peak of J-aggregates does not contribute to carotenoid resonance conditions, and show how the Raman shift of the C=C stretching mode is dependent on both, the molecular environment and the excitation wavelength. Overall, the spectroscopic data collected here is highly relevant for the interpretation of *in situ* spectroscopic data in terms of carotenoid identification and quantification by resonance Raman spectroscopy as well as the preparation of reference samples. In particular, our data promotes careful consideration of appropriate molecular environment for reference samples. https://doi.org/10.1063/1.5025788

I. INTRODUCTION

One promising application of optical spectroscopy is the *in vivo* analysis of the carotenoid content of human tissue[1,2] or plants.[3] Carotenoids play a key role in photosynthesis[4] and are an important class of molecules in human tissue[5,6] - mainly in antioxidant defense. As carotenoid deficiency in humans may have considerable impact on human health or indicate a health issue, application of optical spectroscopy to assess carotenoid status via the human skin has been promoted in recent years. Both reflectance and resonance Raman spectroscopy have already been applied for this task.[2,7] While reflectance spectroscopy makes use of the absorption spectrum, i.e. the electronic transitions and their fine structure, to identify and analyze molecules, Raman spectroscopy utilizes the vibrational fingerprint of a molecule. The Raman spectrum of a particular molecule generally is independent of the excitation wavelength. However, if the energy of the scattered photon matches the energy of an electronic transition of the molecule, absorption and scattering cross sections of the chromophore are strongly increased and so is the intensity of specific lines in the respective Raman spectrum. This resonance effect may enhance the Raman spectrum by several orders of magnitude. In this way, molecules can be detected even at low concentrations despite the fact that Raman scattering is an extremely weak process by itself. Besides, target molecules may be deliberately selected and enhanced above others based on their resonance behavior. Both the Raman resonance behavior and the absorption spectrum of a molecule are closely connected to the electronic transitions of the

[a]Electronic mail: merve.wollweber@hot.uni-hannover.de

target molecule, so they are both likely to change depending on the molecular environment of the molecule.

In general, simplified and well defined artificial samples are created in order to demonstrate and verify the analytic power of a spectroscopic method for *in vivo* studies such as the analysis of the carotenoid content of living tissues. The standard simplified reference sample for the analysis of the carotenoid content of human skin is a solution of β-carotene in an anorganic solvent, e.g. ethanol. However, as carotenoids are mostly found in the lipid membranes of the cells and any tissue mainly consists of water, emulsions or aqueous solutions may be considered a more realistic, i.e. physiological, alternative. In even more complex cases, when the reference sample needs to represent also the inhomogeneity of the tissue, liquid samples can be replaced by hydrogels, for example to comply with inhomogeneous optical properties of skin tissue or concentration differences in different skin layers. For multimodal analysis, which has become more and more popular in recent years, requirements get increasingly complex as several optical or even non-optical methods may be involved and need to be considered. Consequently, decision on how to properly prepare an optimal reference sample for identification and quantification of carotenoids in human tissue or plants will be based on how well the optical properties of the real target tissue can be reproduced and how well and reproducible the reference sample can be produced. Preparing a solution of β-carotene in ethanol is straight forward but introduction of β-carotene in an aqueous environment such as a hydrogel phantom is not, as crystalline β-carotene (powder) is insoluble in water and, consequently, in most hydrogel base solutions. It is also important to notice that the spectral properties of the carotenoid are significantly affected by the method used for hydrogel production and its parameters, one factor being that β-carotene is prone to degradation by oxidation altering its optical properties over time. Apart from stability aspects, the Raman specific response is also expected to be significantly affected by the aqueous environment in the hydrogel.

In this work, we study the absorption spectrum, the Raman spectrum and resonance behavior of β-carotene in aqueous solutions of ethanol and dilutions of a β-carotene emulsion by water or ethanol and discuss implications on their use as reference samples for the analysis of the carotenoid content of human skin or plants via absorption or Raman spectroscopy. To pave the way for more complex reference samples like tissue phantoms, we also include a poly(vinyl alcohol) hydrogel stained with β-carotene in our studies. This phantom material was chosen because of its versatility allowing application for both optical and acoustic measurement techniques.[8]

II. MATERIALS AND METHODS

A. Sample preparation

For experiments on β-carotene in water-ethanol mixtures, a stock solution of β-carotene (Carl Roth, Germany) in ethanol (HPLC grade, Carl Roth, Germany) was prepared. The concentration of the stock solution was close to saturation. The stock solution was diluted by water in a step by step manner down to below 20% ethanol in water allowing for measurement of absorption spectra at each step.

For experiments on β-carotene in a lipid environment with varying ratios of water and ethanol, a stock solution containing 32 mg of an emulsion of β-carotene (Altratene 5% EM, 5.9% emulsion) in 100 mg water was used. This stock solution was then further diluted by ethanol step by step to allow for measurement of absorption spectra in a molecular environment in the range of 42-75 % ethanol.

For preparation of poly(vinyl alcohol) (PVA) hydrogels containing β-carotene, the well-known protocol described by Kharine et al.[9] was modified. PVA (20 %wt/wt) was dissolved in demineralized water. The solution was prepared in a water bath at 95 °C and stirred continuously during the process. In the next step, ethanol was added to obtain a clear hydrogel after one single freeze-thawing cycle. This deviation from the original procedure where dimethyl sulfoxide (DMSO) is added as anti-freezing and pro-polymerization agent is an important improvement for handling and reproducibility of tissue phantoms based on these hydrogels as it allows to produce phantoms without the need of a final rinsing procedure in order to remove the DMSO. The phantoms can be used directly after

thawing and may even be handled without gloves as the hydrogel is non-irritant. In 1992, Takigawa et al.[10] already introduced ethanol in PVA gels, but they performed a complete substitution by first preparing a standard DMSO/water PVA gel, and subsequently drying it and reswell it by ethanol, so their approach differs significantly from the procedure presented and used here. Compared to ethanol, the solubility of β-carotene is better in other organic solvents such as tetrahydrofurane, for example. However ethanol is one of the very few solvents that are non-toxic/non-irritant. Both DMSO and ethanol can be used to introduce β-carotene in a hydrogel, but without a rinsing step, loss of dye molecules that will be washed out with the DMSO or swelling of the hydrogel in the water bath that may cause unwanted increased turbidity of the phantom are avoided. The water:ethanol ratio was varied for experiments. A clear hydrogel is produced with ca. 25-40 %v/v of ethanol in aqueous solution. To obtain carotenoid-stained hydrogels, pure ethanol was either (partly) replaced by a solution of β-carotene in ethanol (30 μg/ml), or an emulsion of β-carotene, Altratene 5% EM (5.9% emulsion), was added. Hydrogels in this study were formulated with 12 %v/v of ethanol. In order to minimize evaporation losses and exposure to oxygen resulting in degradation of the carotenoid, the container was kept closed whenever possible during the whole process. Finally, the solution was cast into 3 cm diameter petri dishes or 10 mm pathlength cuvettes and allowed to stand for about an hour to let air bubbles migrate to the surface. After that, samples were cooled and kept at -14 °C for 12 hours or more for PVA polymerization, then thawed and kept at room temperature for subsequent measurements.

PVA (>99% hydrolyzed) was purchased from Sigma Aldrich, Germany. Ethanol (HPLC-grade) and β-carotene were purchased from Carl Roth, Germany. Altratene 5% EM was kindly provided by Allied Biotech and used as emulsion of β-carotene.

B. Spectrophotometry

Absorption spectra were measured by a spectrophotometer (Uvikon 931, Kontron Instruments) in the ultraviolet and visible wavelength range (full range 190-900 nm). Samples were contained in Suprasil standard cuvettes (10 mm pathlength).

Liquid samples were freshly mixed or shaken prior measurements to ensure homogenous distribution within the sample. For the PVA hydrogels, absorption spectra were measured at several times during processing and storage to determine possible effects of the formulation and production process of the hydrogels on their optical properties - especially with respect to β-carotene.

Peak positions in the absorption spectra were determined by fitting with Gaussian peak shapes.

C. Resonance Raman spectroscopy

For the resonance Raman measurements, an OPO laser system (NL303G + PG122/UV, Ekspla, Lithuania) was used, providing ns-pulses in the wavelength range 210-345 nm and 420-2300 nm. Samples were contained in 10 mm standard suprasil cuvettes. A fiber bundle consisting of a central excitation fibre (800 μm core diameter, NA: 0.22) surrounded by detection fibers (200 μm core diameter, NA: 0.22) was placed centrally in front of the cuvette to excite and detect the Raman scattered light. Raman spectra were recorded by an imaging spectrograph (Shamrock SR 500i, Andor, U.K.) equipped with a CCD-camera (Newton DU940P-BU, Andor, U.K.). A 100 μm entrance slit and a 1200 l/mm grating blazed at 500 nm were used. Rayleigh scattered light was blocked by long-pass filters (RazorEdge, Semrock, U.S.A.).

Resonance Raman spectra are measured by step-by-step tuning of the laser over the (pre-) resonance range of the respective molecule. In this case, 440-534 nm was chosen as suitable for β-carotene and this range was covered in 2 nm steps. All Raman spectra were measured at a repetition rate of 10 Hz by accumulating 200 mJ of excitation light. Single pulse energies were below 10 mJ. No sample heating or spectral artifacts because of accumulation of photoproducts were observed.

An iterative morphological and mollifier-based baseline correction[11] was applied to all Raman spectra. In order to better show the resonant enhancement of the Raman scattering, spectra were rescaled to compensate for the general increase of scattering cross sections with shorter wavelength. The wavelength dependent sensitivity of the detection system hardly changes in the resonance range

of β-carotene: it rises by less than 4% from above 460 nm to 534 nm. So, Raman intensities were not corrected for the spectral sensitivity of the detection system.

Data is processed in the form of resonance maps, i.e. excitation-emission matrices, and as resonance profiles showing the dependency of the Raman intensity of a single line on the excitation wavelength. To cover the fingerprint region of β-carotene at high spectral resolution, an optimal grating position of the spectrograph for each excitation wavelength needs to be set. Consequently, the grating has to be moved for each excitation step. There are always small deviations between the spectral calibration of different grating positions resulting in a slight wobbling of the Raman line positions in the resonance maps. This effect was compensated by recalibrating the Raman spectra to an internal standard line. For the samples containing ethanol, spectral recalibration to the ethanol Raman line at 884 rel. cm^{-1} was applied. For samples prepared from the β-carotene emulsion, the main C-C stretching mode at 1157 rel. cm^{-1} was used.

Peak positions of Raman lines and resonance profiles were determined by fitting with Lorentzian peak shapes. Gaussian components were neglected as initial fitting with Voigt shapes showed only minimal contributions from Gauss shapes. For the resonance profiles, two close lying peaks were assumed: the main peak for the 0-0 transition and a first fine structure peak.

D. Confocal Raman microscopy

A confocal Raman microscope (CRM200, WITec, Germany) was used to image the distribution of β-carotene, PVA, and water in the hydrogel matrix. Spectra were recorded using a frequency-stabilized, frequency-doubled continuous-wave Nd:YAG laser at 531.9 nm with a standard lens (Nikon 0.55 EWLD LU Plan 50x) and 2 s integration time. Laser intensity before the objective was set to 35 mW resulting in approximately 26 mW on the sample. Visual inspection of the samples after measurement and repetition of measurement showed no significant change of the sample due to heating and accumulation of photoproducts. The system has a spectral resolution of 5 cm^{-1} using a 600 l/mm grating and a slit width of 50 μm, realized by a multimode fiber connecting the Raman microscope to the spectrometer (UHTS 300 by WITec).

Hydrogels with and without β-carotene were measured in their liquid form before freeze-thawing and after polymerization. Color coded images were prepared by filtering the following spectral regions: 3050-3650 rel. cm^{-1} for water, 910-935 rel. cm^{-1} for PVA, and 1507-1540 rel. cm^{-1} for β-carotene. PVA and ethanol, both constituents of the hydrogel, have quite similar Raman spectra. Their spectra mainly differ in the fine structure of the C-H stretching modes in the range 2800-3100 rel. cm^{-1} which are significantly more pronounced in ethanol while they may even merge to one broad peak in polymerized PVA. However, these characteristics are difficult to implement for spectral analysis and discrimination of the two components. Two weak peaks occur in PVA at 926 cm^{-1} and 1128 cm^{-1} that are not present in ethanol. The former can be assigned to a C-C stretching mode which becomes stronger with increasing hydration of PVA.[12] The latter was proposed to be characteristic for amorphous PVA.[13] The peak at 1128 cm^{-1} can be strongly affected by the close lying C-C stretching peak of β-carotene, so the peak at 926 rel. cm^{-1} is the most reliable peak for imaging PVA distributions despite its relative weakness and so it was chosen as the characteristic PVA Raman line for color coded images of the distribution of the different constituents.

III. RESULTS AND DISCUSSION

As will be detailed in the following subsections, both the absorption spectrum and the Raman resonance behavior of β-carotene are significantly dependent on the molecular environment. As either β-carotene solution in ethanol or β-carotene emulsion are used to prepare β-carotene dyed hydrogels, results are discussed with respect to these two base components.

A. Absorption spectra

1. The basic PVA hydrogel - clear phantoms

Without addition of β-carotene, prepared PVA phantoms are clear and show only a weak PVA absorption peak in the UVC range (data not shown). Accordingly, the PVA matrix of the hydrogels

has no significant contribution to the absorption or elastic scattering properties of a PVA hydrogel based tissue phantom in the visible spectral range.

2. Ethanol solution of β-carotene - aqueous dilutions and hydrogel

In the PVA-hydrogels prepared from an ethanol solution of β-carotene, the carotenoid is exposed to a mixture of PVA, water and ethanol. We observed, that the absorption of β-carotene in the hydrogel is significantly weaker than expected for the respective β-carotene concentration and shows spectral differences compared to pure β-carotene in ethanol solution depending on the water-ethanol ratio.[14]

The general loss of absorbance alone could mainly be attributed to degradation during the hydrogel production process caused by heat and oxidation. Degradation products of β-carotene are characterized by absorption in the near-UV region (330-400 nm) while the visible absorption near the main maxima noticeably weakens, and these oxidation products are dominated by compounds with few conjugated double bonds.[15] Under ambient atmosphere, approximately two thirds of the β-carotene content is degraded and lost in the process. However, no significant spectral shifts are caused by the degradation, but only a weak increase in UVB absorption.

The absorption properties of β-carotene heavily depend on the molecular environment. Fig. 1 shows absorption changes in response to the ratio of water to ethanol. It is well known that a high water content in water-miscible solvents can cause the observed marked decrease in the intensity of the usual main absorption band of carotenoids and leads to the appearance of a new, intense absorption peak usually in the near ultraviolet region.[16] This marked increase in the *cis*-band however is not observed in our experiments. Instead, the fine structure in the visible range changes significantly. New spectral components appear as the ethanol content in the aqueous solution drops below 67%, which is most obvious in the new peak at approximately 518 nm. The energy of the electronic transition that gives rise to the main absorption band of carotenoids depends on the refractive index of the solvent: a larger refractive index causes a shift to lower energy in the absorption band, which appears as a bathochromic shift in the absorption spectrum.[16] The main absorption peak of β-carotene may shift up to 40 nm depending on the refractive index of the solvent or the solvent's polarizability, respectively.[17,18] However, the refractive indices of the hydrogel components are quite similar. Water has a refractive index at 589.29 nm (n_D) of 1.33, ethanol of 1.36, and n_D of a 15-20% wt/wt solution of PVA in water is 1.35. Furthermore, the quite abrupt changes in the spectral characteristics at certain levels of water:ethanol ratio are in contrast to the gradual change of refractive index in the solution.

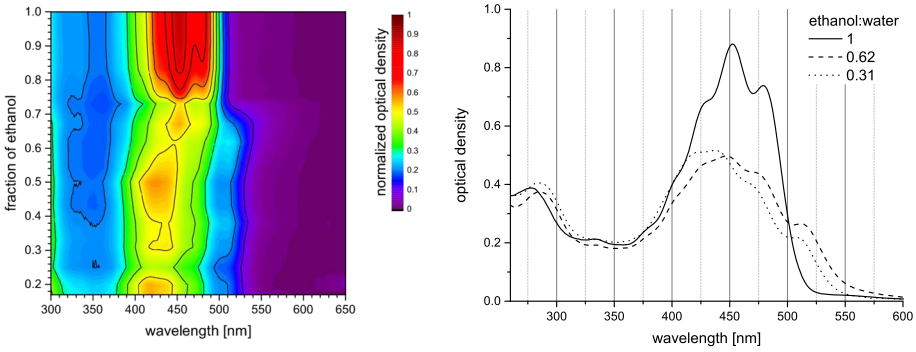

FIG. 1. Changes in the absorption spectrum of β-carotene in solution depending on the ratio of ethanol to water. All spectra were normalized to the same β-carotene concentration assuming linear dependency of optical density on concentration. Left: spectral changes mapped for β-carotene solved in various ratios of ethanol and water from pure ethanol to less than 20% ethanol in aqueous solution. Right: three spectra from this series of measurements to give a more detailed impression of the spectral differences observed. Pure ethanol solution shows the characteristic spectrum and fine structure of β-carotene with peaks or shoulders, respectively, at approximately 429 nm, 452 nm and 479 nm. Absorption decreases gradually with increasing water content in the solution. As the ethanol content drops below 67%, the shape of the absorption spectrum changes abruptly as a new red-shifted peak appears. Reproduced with permission from Meinhardt-Wollweber *et al.*, SPIE 89450B (2014). Copyright 2014 Society of Photo-Optical Instrumentation Engineers (SPIE).

The water:ethanol ratio also affects the solubility of β-carotene, as β-carotene tends to form aggregates in aqueous solution below a critical fraction of ethanol. The concentration of β-carotene in the ethanol stock solution is already close to saturation. The solvent:water ratio at the observed appearance of the additional red-shifted peak is in good agreement with the findings of Hempel et al.[19] studying formation and spectral absorption properties of β-carotene in hydrated acetone solutions. They spot spectral features characteristic of J-aggregates above 40% water, increasing water content in 20% steps. However, vibrational fine structure is better maintained in acetone-water mixtures. In dried thin films, they found a spectral distance of 40 nm between the longest wavelength absorption peaks (487 nm and 528 nm). An equal but shifted spectral spacing is found in our experiments (479 nm and 518 nm). For zeaxanthin, a very similar carotenoid, the absorption spectra of J-aggregates but not H-aggregates also show the additional red peak observed here for β-carotene and an overall similar spectral structure.[20] Therefore, the observed effects are probably due to aggregation of the carotenoids. Hager[21] found a similar spectral behavior for β-carotene extracted from spinach chloroplasts in dependence on the water:ethanol ratio pointing out that the carotenoid is still solved. So, though small carotenoid complexes may have formed, no large complexes, i.e. carotenoid colloids, appeared. The carotenoid concentration in Hagers' experiments was 3,95 μg/ml.

3. β-carotene emulsion - aqueous dilutions and hydrogel

In emulsion, β-carotene is exposed to a lipid-water environment. As shown in Fig. 2, absorption maxima of β-carotene appear at approximately 466 nm and 497 nm under these conditions. With increasing ethanol content, the β-carotene spectrum gains features of aggregated β-carotene (compare section III A 2) to finally show characteristics similar to β-carotene in pure ethanol. The solubility of β-carotene in lipids (>1 g/l)[22] is much higher than in ethanol (30 mg/l).[23] Consequently, a much more intense stain can be achieved in aqueous dilutions or hydrogel phantoms prepared from emulsion.

Hager[21] reports the loss of spectral fine structure accompanied by the appearance of a red shifted absorption peak (and/or an additional UVA peak) for carotenoid complexes and aggregates in the presence of water and lipids. Besides, exemplary carotenoid absorption spectra from intact chloroplasts also show the spectral characteristics of carotenoid complexes indicating that carotenoids are found in complexes *in vivo* and that this form and the respective spectra may even be rather typical under physiological conditions.

In tissue, non-polar carotenoids like β-carotene are likely to be located in membranes,[24] so a lipid-water environment similar to that in chloroplasts may be assumed as well. Experimental data on the absorption profile of carotenoids *in vivo* is scarce as it needs to be deduced from whole

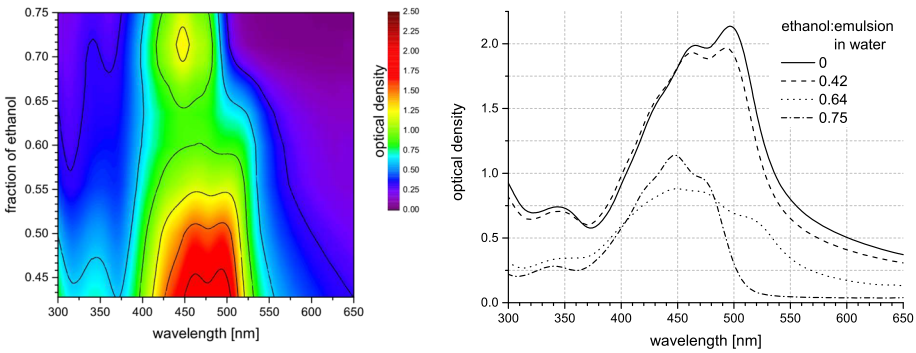

FIG. 2. Absorption spectra of β-carotene emulsion depending on the ratio of ethanol and water. Left: spectral map for β-carotene emulsion in various ratios of ethanol and water from 75% ethanol to ca. 42% ethanol in aqueous solution. Right: three spectra from this series of measurements and an additional spectrum for an emulsion in pure water. Note that pure emulsion in water and ethanol-water dilutions are from different stock solutions of emulsion in pure water (21 mg/100ml for zero ethanol, 32 mg/100 ml for the ethanol dilution series). Reproduced with permission from Meinhardt-Wollweber *et al.*, SPIE 89450B (2014). Copyright 2014 Society of Photo-Optical Instrumentation Engineers (SPIE).

tissue spectra. Andree et al.[25] calculated *in vivo* absorption spectra of skin carotenoids based on a modified reflection model by Zonios and Dimou.[26] After intake of a significant amount of carrot juice, they report an increased absorption of human skin in the range from 450-500 nm. As the prime carotenoid in carrot juice is β-carotene (approx. 3-4 times the amount of contained α-carotene[27]), this spectral change is likely to originate from β-carotene absorption. Comparing absorption spectra from β-carotene in cyclohexane, in carrot juice and in skin, they found that the skin spectrum lacks distinct fine-structure features and is shifted by 10 nm compared to the spectrum in solution. The same 10 nm shift is observed for carrot juice so they conclude that absorption spectra from juice seem to give a more reliable basis spectrum than a β-carotene solution. The broad absorption between 450 and 500 nm agrees well with our data on β-carotene in emulsion, whereas absorption of β-carotene in ethanol is much stronger at 450 nm than at 500 nm.

Accordingly, it seems to be most appropriate to use carotenoids in emulsion rather than in an organic solvent like ethanol in a tissue phantom for absorption spectroscopy. In this way, more physiological optical properties can be achieved, probably also for resonance Raman spectroscopy.

B. Resonance Raman profiles of PVA hydrogels stained with β-carotene

A strong resonance enhancement of Raman scattering can be achieved by chosing an excitation wavelength close to an electronic transition of the target molecule. Due to the close relation of absorption and Raman resonance, the spectral changes in the absorption properties of β-carotene in response to the molecular environment described in section III A are expected to be reflected in the resonance profiles of the Raman spectra as well. Vibronic transitions do not contribute equally to Raman resonance. For β-carotene, the main contribution to resonance enhancement is from the 0-0 transition. In general, this is synonymous with the absorption peak at the long wavelength end.

This is true for ethanol solution where the longest wavelength peak in the absorption spectrum originates from the 0-0 transition of β-carotene. With increasing water content, this peak is slightly blue-shifted and its intensity decreases. The parallel behavior is observed in the resonance profiles of the respective Raman spectra (Fig. 3, top row). The strongest Raman peaks of β-carotene are at approximately 1157 cm^{-1} (C-C stretch) and 1528 cm^{-1} (C=C stretch). At 20% water content (Fig. 3, top row, left), two more carotenoid lines are detected: 1011 cm^{-1} (methyl rocking) and 1195 cm^{-1} (C-C stretch). The concentration of β-carotene in the 40% water solution is approximately 0.7 of that in the 20% solution. The intensity of Raman signals scales linearly with concentration, but the Raman signal difference between the two samples is considerably larger than expected from this effect. More importantly, the differences in absorbance for β-carotene in different molecular environments (see section III A 2) also have a significant effect on the intensities of the resonance Raman signals. Interestingly, the slight spectral shift in the 0-0 absorption peak of the carotenoid monomer can be seen as a blue shift of the resonance profiles as well. It should be pointed out that the additional red-shifted peak in the absorption spectra of solutions with high water content does not influence the spectral position of the resonance.

In the emulsion as well as in the hydrogel stained with emulsion, Raman intensities are strongly increased. Accordingly, more Raman peaks of β-carotene can be seen at approximately 959 cm^{-1} (ring methylene rocking), 1011 cm^{-1} (methyl rocking), 1163 cm^{-1} and 1195 cm^{-1} (C-C stretch), and around 1528 cm^{-1} (C=C stretch) (see Fig. 3, bottom row); mode assignment was done according to Tschirner et al.[28] Even though the β-carotene concentration used in these samples is only ca. 20% higher than that in the 20% water-ethanol solution, Raman intensities more than double. The increase in absorbance, however, is even larger than the resonance increase of the Raman signals. Resonance maxima are red-shifted by more than 20 nm compared to ethanol solution, which also matches well with the observations in the absorption spectra.

Contribution of carotenoid degradation products to the Raman spectra is not expected as the absorption and consequently the resonance condition of these compounds is shifted to the ultraviolet wavelength range.[15]

Figure 4 and Table I give a synopsis of the spectral characteristics and shifts of β-carotene absorption and resonance Raman scattering profile in the different molecular environments.

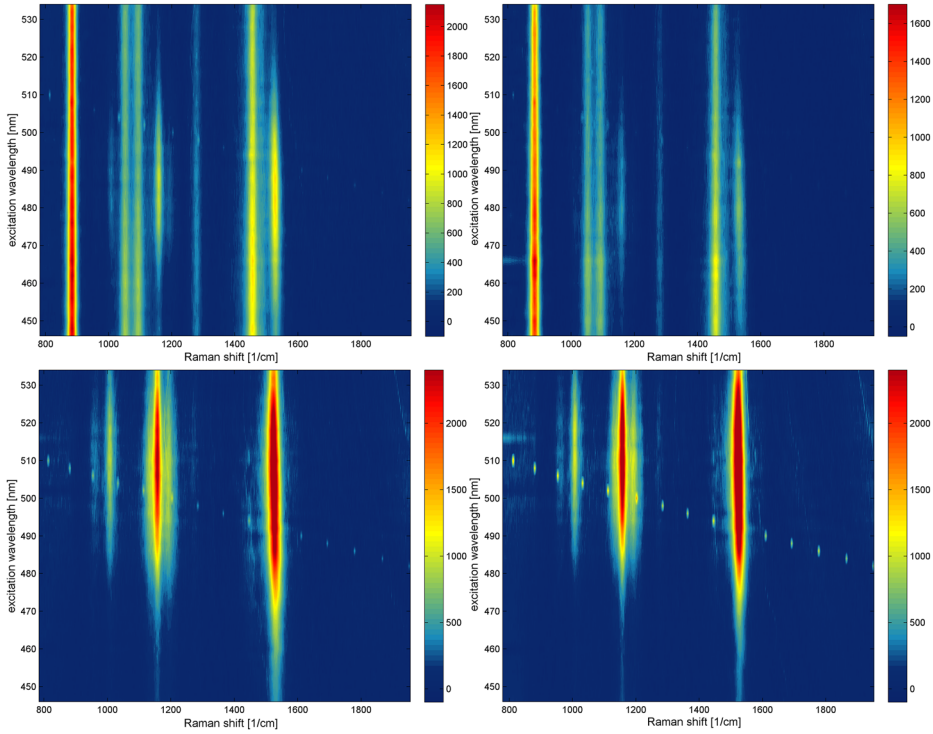

FIG. 3. Resonance Raman maps for β-carotene in different molecular environments. Raman spectra are mapped for excitation wavelengths between 446 and 534 nm. Raman intensities are color coded. Top row, left to right: ethanol solutions with 20% and 40% water content. Bottom row: resonance maps for 64 mg Altratene EM5% emulsion in 100 ml of water (left) and a PVA hydrogel stained with 11 mg Altratene EM5% emulsion in 100 ml of aqueous solution (<12% ethanol) (right). Carotenoid Raman peaks can be seen at 959 cm^{-1} (ring methylene rocking), 1011 cm^{-1} (methyl rocking), 1163 cm^{-1} and 1195 cm^{-1} (C-C stretch), and around 1528 cm^{-1} (C=C stretch). In ethanol solution, the peak at 959 cm^{-1} is missing and the peaks at 1011 cm^{-1} and 1163 cm^{-1} drop below detection limit in the 40% water solution. Additional Raman bands in the ethanol solutions (top row) are ethanol Raman peaks. The resonance maxima are approximately the same only for emulsion and hydrogel. Note that the color scales for Raman intensities are different in the different graphs. The diagonal line of artifacts seen in the spectral maps in the bottom row originate from an external light source. Reproduced with permission from Meinhardt-Wollweber *et al.*, SPIE 89450B (2014). Copyright 2014 Society of Photo-Optical Instrumentation Engineers (SPIE).

C. Raman peak positions

In this work, Raman spectra of β-carotene were measured at a wide range of (pre-)resonance conditions (440-534 nm) and in different molecular environments studying their influence on Raman resonance conditions and line positions to enable a well informed choice of experimental conditions for reference samples.

Hayashi et al.[29] investigated the resonance Raman spectra of carotenoids from bacteria in vivo and as extracts in benzene and found a strong similarity of the *in vivo* and *in vitro* resonance Raman spectra concluding that no significant modifications in the vibronic coupling has been caused by the chromatophore environment. Generally, no change in Raman peak positions is expected in dependence of the molecular environment, i.e. organic solvents or lipids. Peak positions do however depend on carotenoid conformation, e.g. the Raman peak of the C=C stretch vibration of β-carotene may shift up to 10 cm^{-1} in relation to the C-C Raman line comparing the all-*trans* and central-*cis* isomers.[30] Besides, Tschirner et al.[28] found a wavelength-dependent variation of the peak maximum of the C=C stretch vibration for β-carotene in dichloromethane and photosystems I and II[28] that they attributed to different relative resonances of the two underlying modes, and pointed out that their quantum chemical calculations could not reproduce the effect.[28,31] According to their experimental data, the peak maximum shifts from 1525 cm^{-1} at 1064 nm to 1521 cm^{-1} at around 514 nm and up again to 1525 cm^{-1} at 465 nm.

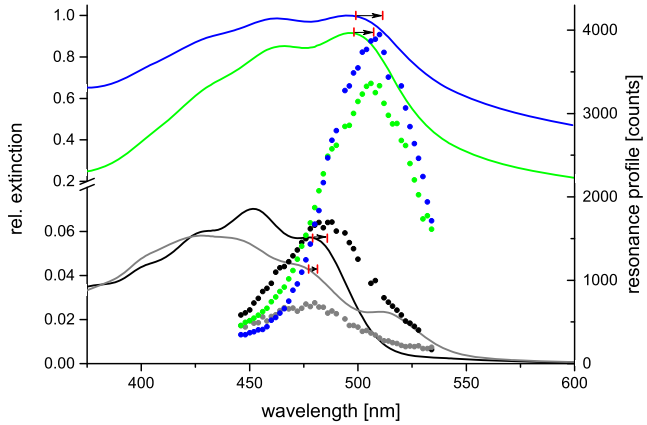

FIG. 4. Absorption (solid lines) and resonance Raman profiles (dots) for β-carotene in different molecular environments. Raman spectra are mapped for excitation wavelengths between 446 nm and 534 nm, and the resonance profile of the strongest carotenoid Raman peak at ca. 1528 cm^{-1} (C=C stretch) is displayed here. From top to bottom, the curves show resonance maps for 64 mg Altratene EM5% emulsion in 100 ml of water (green), a PVA hydrogel stained with 11 mg Altratene EM5% emulsion in 100 ml of aqueous solution (<12% ethanol) (blue), ethanol solutions with 20% (black) and 40% (gray) water content. Distance marks (arrows) at the 0-0 transition peak indicate how far absorption and resonance maximum are displaced for each sample.

Figure 5 shows this variation for our data as extracted from the Raman profiles shown in Fig. 3 where they appear as a slight incline in the C=C stretch Raman line over the excitation range. The dependence of the peak positions of β-carotene on the molecular environment was not in the focus of this study, so our data is limited. However, we observe a minimal Raman peak position of approximately 1523 cm^{-1} at excitation around 523 nm for the emulsion based samples. The peak position shifts up to 1528 cm^{-1} at 476 nm and 1530 cm^{-1} at 474 nm, respectively. Whether this is the maximal peak position cannot be clarified from our data, so we can only state a peak shift of at least 5-7 wavenumbers within the resonance range. In the ethanol water mixtures, we observe considerably larger variation of the peak positions depending on the excitation wavelength and the solvent conditions. For the sample containing 20% water, the C=C peak position shifts from 1525 cm^{-1} at 500 nm to 1529 cm^{-1} at 450 nm. For the sample containing 40% water, a shift from 1525 cm^{-1} at 514 nm to 1536 cm^{-1} at 446 nm was found. It is not clear from our data whether C=C line shifts even further up or down beyond the excitation range studied here. Still, it is noteworthy that the observed

TABLE I. Absorption maximum relevant for resonance (0-0 transition) and resonance peak of the C=C Raman line. Peak positions were determined by fitting of the spectra with a linear combination of multiple Gaussian peaks for absorption and two Lorentz peaks for the resonance profiles. Standard errors of the fits are given as well. Note that the position of absorption and resonance peaks also differs relatively to each other as can be read from their spectral distance; EM: emulsion in 100 ml of water, 80:20: ethanol solution with 20% water, 60:40: ethanol solution with 40% water (in the last case, not the 0-0 transition of the aggregate but the longest wavelength peak of the central carotenoid absorption band is considered.

sample	0-0 peak [nm]	std. error	Resonance peak [nm]	std. error	Distance [nm]
EM	498.2	0.3	507.3	0.5	9.1
PVA hydrogel	500.0	2.5	511.4	1.5	7.1
80:20	479.1	0.3	485.8	0.8	6.7
60:40	477.2	1.6	481.3	4.8	4.1
sample	1 ← 0 peak [nm]	std. error	Resonance peak [nm]	std. error	Distance [nm]
EM	461.0	1.3	485.4	0.6	24.4
PVA hydrogel	460.8	8.0	491.9	1.1	31.1
80:20	452.0	1.0	459.4	2.8	7.4
60:40	453.3	1.6	459.1	35.4	5.8

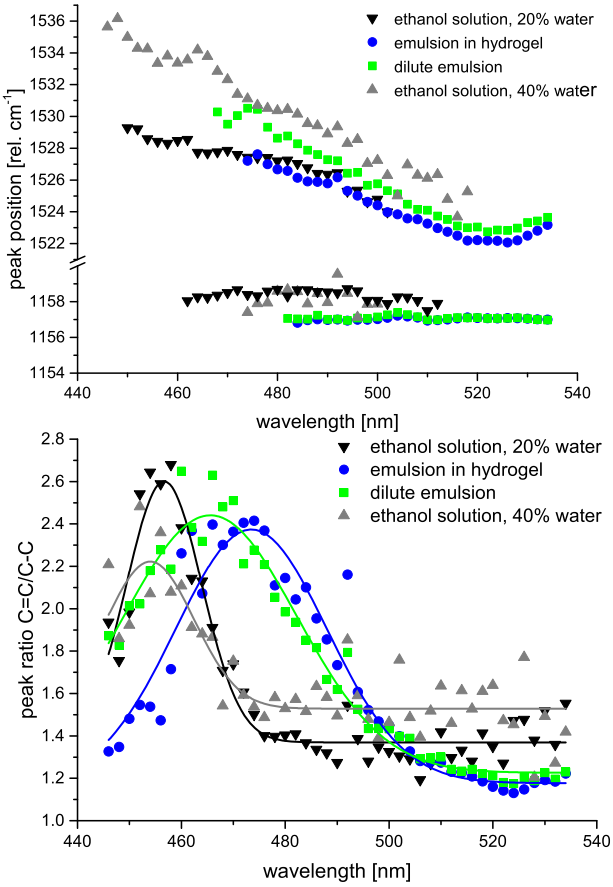

FIG. 5. Dependence of peak positions (*top* panel) and intensity ratios (*bottom* panel) of the C-C (1157 cm^{-1}) and C=C (around 1528 cm^{-1}) stretch vibrations of β-carotene on the excitation wavelength in different molecular environments. Note that all spectra were spectrally recalibrated to the C-C vibration at a Raman shift of 1157 cm^{-1} (see Sec. II C), so peak-to-peak distances but not absolute peak positions are reliable. Lines in the graph presenting the peak intensity ratios were included to guide the reader's eye. Data is shown for 64 mg Altratene EM5% emulsion in 100 ml of water (green), a PVA hydrogel stained with 11 mg Altratene EM5% emulsion in 100 ml of aqueous solution (<12% ethanol) (blue), ethanol solutions with 20% (black) and 40% (grey) water content.

shift of the C=C peak is more than 10 cm^{-1} for the sample with 40% water content, while the shift is less pronounced (4 cm^{-1}) in the sample containing less water; so the line positions move apart towards their maximal shift in the blue range.

Banerjee et al.[32] revisited the C=C Raman line shift experimentally found by Tschirner et al.[28,31] calculating resonance Raman spectra of β-carotene with a more comprehensive model also accounting for Duschinsky rotation. They found that upon inclusion of the Duschinsky effect, the Raman spectra of carotenoids are sensitive to wavelength dependent mode mixing in the resonance range. Even though (quantitative) comparison of our experimental data with the theoretical results of Banerjee et al.[32] is difficult, apparently, we observe larger shifts of the C=C Raman lines than predicted by their theoretical approach. Banerjee et al.[32] also calculated relative peak intensities for several Raman modes. Peak ratios for the C=C vs the C-C peak are shown in Fig. 5 for our experimental data. Interestingly, our intensity ratios are in better agreement with the calculations from Banerjee et al.[32] not including Duschinsky rotation: They compared peak intensities for these two lines at 496 nm and 454 nm excitation predicting that the line originating from C=C stretching mode is stronger than the C-C stretching line at 496 nm while it is the other way around at 496 nm. When Duschinsky rotation is not included, only a moderate dependence of peak intensity ratios on the excitation wavelength is predicted and the C=C line is the strongest line at both excitation conditions.

Another interesting detail is the difference in C=C peak position between the two ethanol-water solutions. The absorption spectrum of the 40% water solution clearly shows a red-shifted extra peak as characteristic for J-aggregate formation which is not present in the 20% water solution (see Fig. 4). Salares et al.[33] found that the C=C peak position of carotenoid aggregates is shifted by ca. 6 cm^{-1} to lower wavenumbers compared to its unaggregated form. For Zeaxanthin, Wang et al.[20] report downshifts of 3-9 cm^{-1} for the C=C Raman line upon aggregation. Ishigaki et al.[34] studied lycopene aggregates finding only 1 cm^{-1} shifts between monomer and aggregates. For β-carotene, however, we observed quite the opposite effect: the C=C Raman line appears to shift to higher wavenumbers by up to 6 cm^{-1} upon aggregation.

D. Distribution of carotenes in the hydrogel

As reported in the previous sections, the molecular environment of the carotenoids is crucial for their optical properties as the microenvironment and possible aggregation may have a strong impact on carotenoid absorption and thus Raman resonance. In a tissue phantom, the carotenoids are exposed to both water and ethanol as well as the PVA matrix. For the phantoms stained with carotenoid emulsion, the lipid environment is expected to play an additional important role.

In order to investigate the microenvironment of the carotenoids in the hydrogel, we analyzed carotenoid, water and PVA distribution in the PVA hydrogels pre and post polymerization with confocal Raman microscopy (532 nm excitation). The lipids of the emulsion were below the detection limit of the confocal Raman microscope, so their distribution is not known. However, the characteristics of the absorption spectrum of β-carotene in emulsion are mostly conserved in the stained hydrogel, indicating that the molecular environment of β-carotene has not changed significantly from emulsion to embedding in the hydrogel. While water and carotenoids can be identified unambiguously by their Raman signal, PVA and ethanol share most of their Raman lines and are thus difficult to discriminate. PVA can be identified by an additional though weak line at 926 rel. cm^{-1} which is not present in the ethanol signal. Ethanol on the other hand does not show unique lines compared to PVA, so it was not possible to determine and analyze its distribution.

As expected, water was evenly distributed in the hydrogels and the polymer matrix showed a consistent micropattern in all hydrogel samples whether stained or not. All hydrogels were produced by a single freeze-thaw cycle. According to Willcox et al.,[35] the morphology of such gels is characterized by a dense network of pores with 500-1000 nm diameter which are rounded or filled by fibrillar structures during aging (or with increasing number of freeze-thaw cycles). So, the observed micropattern is in good agreement with this literature data given the focus dimensions of the confocal microscope used for these images leading to approximately 300 nm lateral and 1-2 μm axial resolution. Close to the hydrogel surface, i.e. within the first few micrometers, the PVA signal intensity is generally slightly increased. This is probably due to a denser polymer network at the surface. Despite an overall homogeneous color of the hydrogels on the macroscopic scale, the β-carotene distribution is inhomogeneous and sometimes clearly structured at the microscale. Fig. 6 shows examples of microstructures that were found in the hydrogels stained with β-carotene solved in ethanol and β-carotene in emulsion.

Obviously, β-carotene is distributed inhomogeneously in the hydrogel and rather agglomerates in micro streaks or micro globular patches. In the hydrogel stained with emulsion (Fig. 6, double image at the bottom right), the variability of β-carotene concentration is most clearly seen. Here, a β-carotene Raman signal is present in each point of the image. However, there are extended patches with increased intensity, approximately one order of magnitude higher than the carotene background signal. Single spots generally consisting of only 1-3 pixels each yield Raman signal intensities which are several orders of magnitude stronger than the background signal. These hotspots are assumed to originate from unsolved or aggregated clusters with sizes of around 1 μm or below. Comparison of the Raman signals from gels before and after polymerization show that total Raman intensities from β-carotene decrease by more than one order of magnitude for both ethanol solution and emulsion stains during polymerization. The reason for the decay very probably is not the polymerization process itself but rather the time the polymerization takes. In general, stained hydrogels that are exposed to air lose their colour gradually within days (ethanol solution) or several weeks (emulsion) (data not shown).

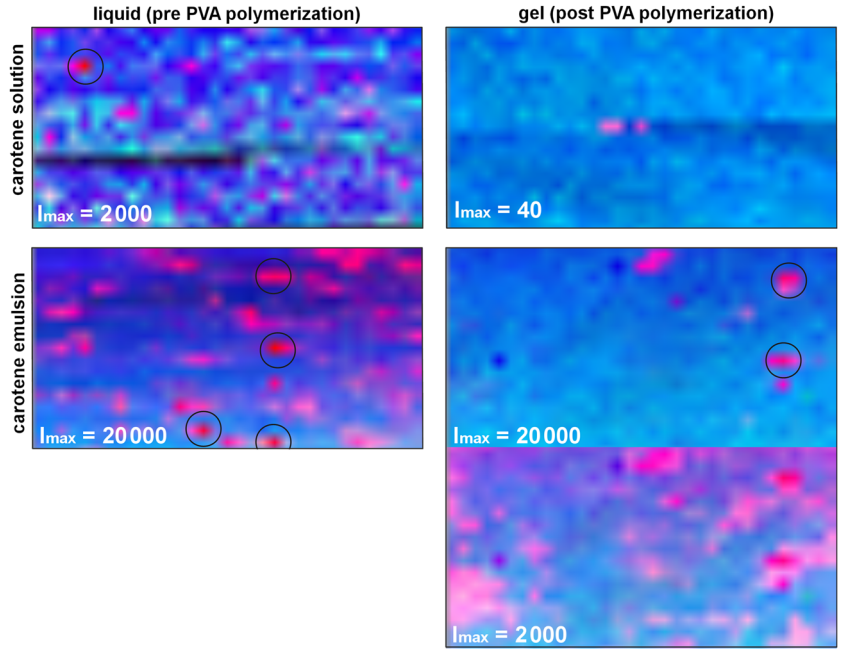

FIG. 6. Raman images of liquid (left) and polymerized (right) PVA hydrogels that were stained with β-carotene solved in ethanol (top) or β-carotene in emulsion (bottom). Water is color-coded in blue and PVA in green yielding turquoise for the hydrogel matrix. The distribution of β-carotene is shown in red. As color saturation encodes signal intensity, carotene distribution appears as different shades of pink in dependence of the β-carotene concentration. Note that full color saturation refers to different maximal carotenoid signal intensities I_{max} (a.u.) in the different images. Circles mark carotenoid agglomerations where exceptionally high β-carotene concentration and very weak water and PVA concentrations are found. The double image at the bottom right shows the same image (polymerized PVA hydrogel stained with β-carotene in emulsion) at two different carotenoid color scales to illustrate the large local variability of β-carotene concentration in the hydrogel. Each image shows a 100 μm wide subsurface area of the gels.

IV. CONCLUSION

We studied the absorption and Raman spectral characteristics of potential β-carotene reference samples for *in vivo* measurements in tissue or plants exposing β-carotene to molecular environments composed of ethanol, water and/or lipids. We paid additional attention to the preparation of β-carotene stained hydrogels that may form a basis for more complex tissue phantoms. Such reference samples are an important tool for validation and calibration of spectroscopic analysis for *in vivo* application.

We showed the well known strong dependence of the absorption spectrum of β-carotene on the molecular environment and how this behavior translates to the resonance profiles of the Raman scattering. In changed molecular environments, absorption and Raman resonance spectrally shift in the same direction, and the offset between 0-0 transition and resonance peak slightly changes. The Raman resonance profiles even show a weak fine structure. It is not clear, whether these secondary peaks originate from the $1 \leftarrow 0$ transitions in the respective absorption spectrum. If so, it is noticeable that in the emulsion based samples, the offset between absorption peak and resonance peak is significantly larger than observed for the 0-0 resonance. Importantly, the characteristic red-shifted absorption peak of J-aggregates does not lead to red-shifted resonance conditions.

Ethanol solution of β-carotene can be used to equip hydrogel phantoms with β-carotene. The fairly high degradation of β-carotene in the production process and spectral changes due to the presence of water have to be considered though, as well as the relatively poor longterm stability of the dye in the hydrogel. Better stability was observed for samples prepared from β-carotene in emulsion. The emulsion used in the experiments contains an additional antioxidant agent (α-tocopherol) to scavenge oxidation and minimize carotenoid degradation. Furthermore, β-carotene concentration is much higher in the emulsion, so scaling of optical properties and concentration

values as desired for a reference sample is facilitated. The strong dependence of the Raman resonance profiles and absorption profiles of β-carotene - or potentially any other carotenoid - on the molecular environment is important for the preparation of reference samples for *in vivo* absorption or resonance Raman measurements. As underscored by the spectra shown in this article, solvent conditions should to be well-considered and well defined in order to avoid misinterpretation of *in vivo* data. This is especially true when resonance Raman spectroscopy is applied for quantification of carotenoids *in vivo*. Gellermann et al. extensively studied this application of Raman spectroscopy: The measurement of total carotenoid content via resonance Raman spectroscopy was validated via reference to HPLC analysis for fruit and vegetable extracts.[36] For analysis of multiple Raman components, reference spectra are used for calibration in the quantification analysis and excitation is often done at a single or only a few different excitation wavelengths. For Raman spectroscopy of carotenoids in human skin, one or two laser lines of the Ar^+-laser are generally used. As the Raman signals of the two main carotenoids in human skin, β-carotene and lycopene, can both be resonantly enhanced using the line at 488 nm, this wavelength is most commonly used. For the discrimination of the two carotenoids, measurements at a second wavelength (514.5 nm) are additionally carried out. In order to calculate carotenoid concentrations from the Raman spectrum, Resonance Raman scattering cross-sections for β-carotene and lycopene under 488 and 514.5 nm excitations are deduced from solutions of beta-carotene and lycopene in ethanol.[1] For discrimination of carotenoids in natural mixtures, our results may be applied to increase the discriminant power and quantitative accuracy of the Raman measurement. In ethanol, the 0-0 transitions for β-carotene and lycopene result in absorption peaks at 478 nm and 504 nm respectively. In this work, we showed that for β-carotene both the 0-0 absorption peak and the respective resonance peak are red-shifted by approximately 20 nm in a lipid environment. Fortunately, in this case, (pre-)resonance excitation is still possible at these conditions even though resonance enhancement is halved for β-carotene according to our data. Solution of carotenoids in pyridine is expected to reproduce spectral characteristics of carotenoids embedded in biological materials quite well,[37] so it can be used if solution in organic solvents is preferred over β-carotene emulsion. Pyridine causes a bathochromic shift of carotenoid absorption spectra by 18-24 nm compared to the spectral positions in ethanol for example.[38]

In summary, if the molecular environment of the carotenoid and its conformation *in situ* is not known, we propose to use β-carotene in emulsion as the basis for a reference sample. First of all, because β-carotene is generally located in membranes within tissue or plants. Secondly, because the proportion of water to ethanol allows to select the molecular environment of β-carotene and thus tune its spectral characteristics within certain limits. Anything from non-polar environment in the lipid vesicles of the emulsion over aggregated forms to the polar environment in mixtures with a high proportion of ethanol is possible with this approach. It also works if a hydrogel is used as the reference matrix, even though extreme conditions strongly influence the mechanical and optical properties of the hydrogel: with decreasing concentration of ethanol in the hydrogel, the phantom becomes more turbid during polymerization for equal freezing temperatures whereas very high ethanol concentrations lead to malformation of the hydrogel.

ACKNOWLEDGMENTS

This work was partly supported by the German Research Foundation (DFG, grant no. WO 1641/2-1). The publication of this article was funded by the Open Access fund of Leibniz Universität Hannover.

[1] M. E. Darvin, I. Gersonde, M. Meinke, W. Sterry, and J. Lademann, Journal of Physics D: Applied Physics **38**, 2696 (2005).
[2] I. V. Ermakov and W. Gellermann, Archives of Biochemistry and Biophysics **572**, 101 (2015).
[3] M. Koch, S. Zagermann, A.-K. Kniggendorf, M. Meinhardt-Wollweber, and B. Roth, Journal of Raman Spectroscopy **48**, 686 (2017).
[4] B. Demmig-Adams, A. M. Gilmore, and W. W. Adams III, FASEB Journal **10**, 403 (1996).
[5] J. T. Landrum and R. A. Bone, Archives of Biochemistry and Biophysics **385**, 28 (2001).
[6] C. O. Perera and G. M. Yen, International Journal of Food Properties **10**, 201 (2007).
[7] E. V. Efremov, F. Ariese, and C. Gooijer, Analytica Chimica Acta **606**, 119 (2008).
[8] B. W. Pogue and M. S. Patterson, Journal of Biomedical Optics **11**, 41102 (2006).
[9] A. Kharine, S. Manohar, R. Seeton, R. G. M. Kolkman, R. A. Bolt, W. Steenbergen, and F. F. M. de Mul, Physics in Medicine and Biology **48**, 357 (2003).

[10] T. Takigawa, H. Kashihara, K. Urayama, and T. Masuda, Polymer **33**, 2334 (1992).
[11] M. Koch, C. Suhr, B. Roth, and M. Meinhardt-Wollweber, Journal of Raman Spectroscopy **48**, 336 (2017).
[12] P. S. Thomas and B. H. Stuart, Spectrochimica Acta Part A: Molecular and Biomolecular Spectroscopy **53**, 2275 (1997).
[13] R. Iwamoto, M. Miya, and S. Mima, Journal of Polymer Science: Polymer Physics Edition **17**, 1507 (1979).
[14] M. Meinhardt-Wollweber, C. Suhr, A.-K. Kniggendorf, and B. Roth, SPIE 89450B (2014).
[15] A. B. Gagarina, N. M. Evteeva, and A. G. Kozyreva, Russian Journal of Physical Chemistry B **2**, 547 (2008).
[16] G. Britton, in *Carotenoids*, edn G. Britton (Birkhäuser, Basel, vol. 1B) pp. 13–62, 1995.
[17] T. Abe, J.-L. M. Abboud, F. Belio, E. Bosch, J. I. Garcia, J. A. Mayoral, R. Notario, J. Ortega, and M. Ross, Journal of Physical Organic Chemistry **11**, 193 (1998).
[18] I. Renge and E. Sild, Journal of Photochemistry and Photobiology A: Chemistry **218**, 156 (2011).
[19] J. Hempel, C. N. Schädle, S. Leptihn, R. Carle, and R. M. Schweiggert, Journal of Photochemistry and Photobiology A: Chemistry **317**, 161 (2016).
[20] C. Wang, C. J. Berg, C.-C. Hsu, B. A. Merrill, and M. J. Tauber, Journal of Physical Chemistry B **116**, 10617 (2012).
[21] A. Hager, Planta **91**, 38 (1970).
[22] P. Borel, P. Grolier, M. Armand, A. Partier, H. Lafont, D. Lairon, and V. Azais-Braesco, Journal of Lipid Research **37**, 250 (1996).
[23] N. E. Craft and J. H. Soares, Journal of Agricultural and Food Chemistry **40**, 431 (1992).
[24] J. D. Johnson, Free Radical Biology & Medicine **47**, 321 (2009).
[25] S. Andree, C. Reble, and J. Helfmann, Photonics & Lasers in Medicine **2** (2013).
[26] G. Zonios and A. Dimou, Optics Express **14**, 8661 (2006).
[27] B. Bao and K. C. Chang, Journal of Food Science **59**, 1155 (1994).
[28] N. Tschirner, M. Schenderlein, K. Brose, E. Schlodder, M. A. Mroginski, C. Thomsen, and P. Hildebrandt, Physical Chemistry Chemical Physics **11**, 11471 (2009).
[29] H. Hayashi, T. Noguchi, M. Tasumi, and G. H. Atkinson, Biophysical Journal **60**, 252 (1991).
[30] Y. Koyama, I. Takatsuka, M. Nakata, and M. Tasumi, Journal of Raman Spectroscopy **19**, 37 (1988).
[31] N. Tschirner, K. Brose, M. Schenderlein, A. Zouni, E. Schlodder, M. A. Mroginski, P. Hildebrandt, and C. Thomsen, Physica Status Solidi (B) **246**, 2790 (2009).
[32] S. Banerjee, D. Kröner, and P. Saalfrank, The Journal of Chemical Physics **137**, 22A534 (2012).
[33] V. R. Salares, N. M. Young, P. R. Carey, and H. J. Bernstein, Journal of Raman Spectroscopy **6**, 282 (1977).
[34] M. Ishigaki, P. Meksiarun, Y. Kitahama, L. Zhang, H. Hashimoto, T. Genkawa, and Y. Ozaki, The Journal of Physical Chemistry B **121**, 8046 (2017).
[35] P. J. Willcox, D. W. Howie, K. Schmidt-Rohr, D. A. Hoagland, S. P. Gido, S. Pudjijanto, L. W. Kleiner, and S. Venkatraman, Journal of Polymer Science Part B: Polymer Physics **37**, 3438 (1999).
[36] P. Bhosale, I. V. Ermakov, M. R. Ermakova, W. Gellermann, and P. S. Bernstein, Journal of Agricultural and Food Chemistry **52**, 3281 (2004).
[37] A. Andreeva and M. Velitchkova, Biotechnology & Biotechnological Equipment **23**, 488 (2009).
[38] G. Britton, S. Liaaen-Jensen, and H. Pfander, *Carotenoids* (Birkhäuser Basel, Basel, 2004).